Preprints of the 21st IFAC World Congress (Virtual)
Berlin, Germany, July 12-17, 2020

A comparison of model-based and black-box methods for speed estimation in aircraft

Gianluca Papa * **Mara Tanelli** * **Giulio Panzani** *
Sergio M. Savaresi *

* *Dipartimento di Elettronica, Informazione e Bioingegneria, Politecnico di Milano, Piazza L. da Vinci 32, 20133 Milano, Italy (e-mail: name.surname@polimi.it)*
** *M. Tanelli is also with Istituto di Elettronica e Ingegneria dell'Informazione e delle Telecomunicazioni - IEIIT CNR Corso Duca degli Abruzzi 24, 10129 Torino, Italy*

Abstract: The anti-skid control system in aircraft is confined to the landing-gear subsystem, and, for safety reasons, it must rely on local signals only. Therefore, it can use only two measurements: the wheel speed and the pilot braking pressure request. Therefore, the anti-skid control logics are generally wheel deceleration-based, as the slip cannot be computed since the aircraft speed is not available. The vehicle speed estimation is commonly done in automotive systems, made possible also by the presence of additional sensors usually coming from an Inertial Measurement Unit (IMU). This work explores how the aircraft speed can be estimated using only the landing gear signals, and if the resulting estimate can be accurate enough to be used in closed-loop with a slip-based anti-skid controller. To do so, two estimation approaches are considered: a sliding-mode model-based one, and a black-box approach grounded on recurrent neural networks. Experimental results are shown, witnessing the potential of black-box approaches.

Keywords: Aircraft; anti-skid control; speed estimation; sliding mode; neural networks.

1. INTRODUCTION

The longitudinal velocity is an essential information when dealing with vehicle dynamics control such as braking, traction and steering. Its main use is the computation of the wheel longitudinal slip, which, in the automotive context, is the main controlled variable in braking-related control systems, such as ABS/anti-lock braking systems and ESP (Savaresi and Tanelli, 2010). In general, the longitudinal speed must be estimated from the available on board sensors. In the automotive literature, different vehicle speed estimation approaches have been presented, ranging from fuzzy-logic Kobayashi et al. (1995); Semmler et al. (2002) to extended Kalman Filter Ray (1997) and non-linear observers Alvarez et al. (2002); Yi et al. (2003), to recursive identification methods, Tanelli et al. (2009). In the two-wheeled vehicles context, it is usually estimated via sensor fusion such as Panzani et al. (2012), or ad-hoc signal processing techniques, Savaresi and Tanelli (2010).

In the aeronautical community, safety and certification issues have up to now prevented anti-lock braking systems to employ signals that are non-local to the landing-gear subsystem, where the braking control unit and all the related electronic equipment reside. Therefore, aircraft anti-skid systems are in general deceleration-based, as the only available measurements on the landing gear are wheel speed and braking pressure. Nonetheless, could the wheel slip be available, the aircraft braking systems could experience the same performance development seen in the automotive context, where mixed-slip deceleration controllers, see *e.g.*, Savaresi et al. (2006), have proved to enjoy both performance and safety features that outperform traditional deceleration-based controllers and, under some circumstances, also pure slip-based ones.

The crucial step in setting up a slip-based controller is the longitudinal speed estimation, facing the challenges of having only the wheel speed and the braking pressure to employ for that purpose, and the highly varying landing conditions were, for instance, the effect of the aerodynamic forces makes the vertical load vary from nearly zero at the landing instant to the static load at the end of the maneuver. In this work we address this problem, comparing a model-based with a black-box approach. More specifically, we leverage the work presented in Tanelli et al. (2012), where a Sliding Mode Observer (SMO) was implemented and validated on experimental data. With the proposed observer, road friction conditions can be retrieved as well *via* non linear curve fitting. Such an observer was later considered for use in the aircraft context in D'Avico et al. (2017).

The structure of the paper is as follows. Section 2 states the considered problem and presents the experimental dataset used in this work. Further, Section 3 introduces the landing-gear and aircraft braking dynamics, while Sections 4 and 5 present the model-based and black-box

approaches for the estimation of the longitudinal speed. Finally, Section 6 compares the performance of the two approaches on the experimental data.

2. PROBLEM STATEMENT

As mentioned in the Introduction, the goal is to estimate the longitudinal aircraft velocity, using only the landing gear measurement collected by the Brake Control Unit (BCU), *i.e.*, the applied braking pressure and the wheel rotational speed. The aircraft serving as our case study has two landing gears and a nose wheel on the front, and the BCU has access to the two pressure measurements and the rotational speed of both landing gears wheels. The scheme of the estimation process is summarized in Fig.1. It is worth pointing out that the two landing gears, and

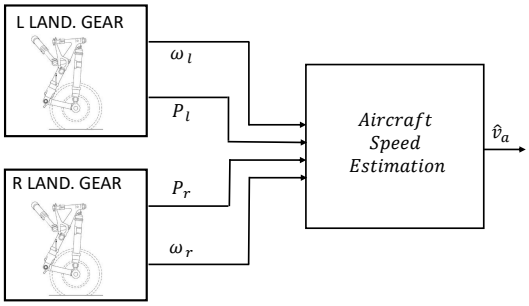

Fig. 1. Conceptual scheme of the aircraft speed estimation algorithm.

consequently the two wheels, experience different stresses and forces during the braking maneuver. This is mainly due to possibly unbalanced working conditions and to the difference in the braking pressures requested by the pilot, who acts on the braking system through a left and right pedal.

We consider and compare two possible solutions to the velocity estimation problem. The first one relies on a model-based approach, and proposes a customized version of the SMO defined in D'Avico et al. (2017), which first estimates the tire-road longitudinal forces, and then retrieves the velocity information from the aircraft longitudinal dynamic model. The second solution explores the potential of black-box approaches, and more specifically investigates the use of a non linear identification method *via* Neural Networks (NNs).

Notably, in both cases, the training, validation and testing of the proposed methods are based on an experimental data set, recorded on test planes from an industrial partner (that is why, for confidentiality reasons, the y-axis scale of plots is usually omitted). The dataset comprises nine different maneuvers, each tagged either as Rejected Take Off (RTO) or landing (LND). Two examples are provided, respectively, in Fig. 2 and 3: the top plot shows the aircraft and wheel speeds, while the bottom one the wheel slips at left and right wheels. The two maneuvers significantly differ, especially because of the load transfer dynamics and thrust force. Indeed, in a RTO maneuver, the aircraft velocity increases while on the ground, and reaches high values in very short time, then for some reasons the take-off is aborted and the aircraft quickly

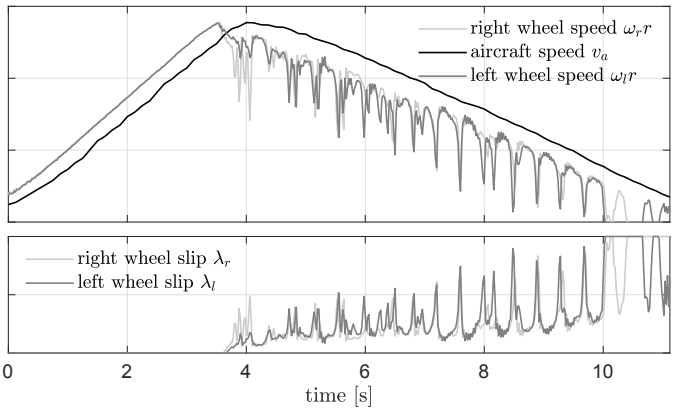

Fig. 2. An example of a RTO maneuver.

breaks in order to cope with the limited left runaway. The commutation between the acceleration and deceleration phases is particularly fast, and this causes large load transfers. In the landing case, instead, the aircraft touches the runway and starts braking until standstill. In this case, the vertical force experiences a very large variation, due to the speed dependent aerodynamic forces. The significant differences in the maneuver motivate the inclusion of instances of both types in the dataset.

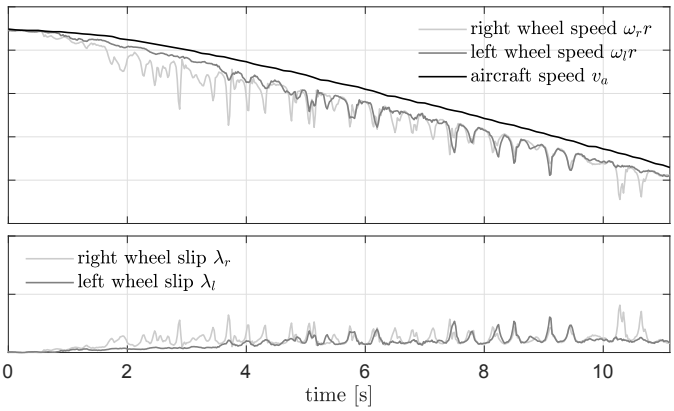

Fig. 3. An example of a LND maneuver.

Moreover, due to the high variability of the aircraft operating conditions, it is important to have an heterogeneous as possible dataset, with respect to aircraft configuration, initial velocity, and road condition. The employed dataset thus includes maneuvers with different aircraft mass and brake-on speed (BOS), *i.e.*, the aircraft speed as the braking commences. The values are reported in Table 1 expressed as percentage variations with respect to their nominal value.

3. LANDING GEAR MODELLING

In order to set up the model-based estimator, a model for the landing gear dynamics is here discussed. It takes into account the gear walk phenomenon (Krüger and Morandini, 2008; Lernbeiss and Plöchl, 2007), an oscillatory motion of the wheel in the longitudinal direction, caused by the elasticity of the landing gear and its peculiar geometry (see Fig. 4). A simple yet expressive way to model this effect is to add to the landing gear a rotational spring-

Table 1. Data set maneuvers specifications: type, mass, BOS.

Man	Type	Mass $[kg]$	BOS $[m/s]$
1	RTO	$+20\%$	-10%
2	RTO	$+14\%$	-50%
3	RTO	-8%	-52%
4	RTO	-8%	-44%
5	LND	-4%	$+14\%$
6	LND	-4%	$+15\%$
7	LND	-8%	$+10\%$
8	LND	$+14\%$	$+30\%$
9	RTO	$+14\%$	$+14\%$

damper component, connecting the aircraft chassis to the vertical axle of the landing gear.

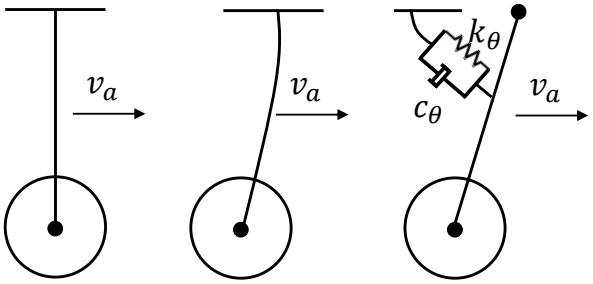

Fig. 4. Schematic representation of the gear walk phenomenon.

The non-linear dynamic model of the landing gear can be written as:

$$(m_a + m_v + m_g v)\dot{v}_a = -F_x - F_{drag} + J_\theta \ddot{\theta} \quad (1)$$

$$J_\theta \ddot{\theta} - J_\theta \dot{v}_a + c_\theta \dot{\theta} + k_\theta \theta = L_{gw} F_x \quad (2)$$

$$J_w \dot{\omega} = r F_x - T_b, \quad (3)$$

where $J_\theta = (\frac{L_{gw} m_{gw}}{2} + L_{gw} m_w), J_\theta \ddot{\theta} = (J_{gw} + \frac{L_{gw}^2 m_{gw}}{4} + L_{gw}^2 m_w)$ and $F_{drag} = \alpha v_a^2$. Equation (1) describes the longitudinal dynamic: the three components on the right hand side F_x, F_{drag} and $J_\theta \ddot{\theta}$ represent the longitudinal contact force, the aerodynamic resistance force, and the inertial component due to the gear walk axle rotation, respectively. Equation (2) models the gear-walk induced rotational dynamics, while Equation (3) accounts for the wheel rotational dynamic, with T_b and rF_x representing the braking torque and the longitudinal tire-road contact force, respectively. As depicted in Fig. 5, the main axle of the landing gear is characterized by the parameters L_{gw}, m_{gw}, J_{gw}, which represent its length, mass and inertia, respectively. The values of the rotational spring/damper, *i.e.*, c_θ and k_θ, can be experimentally tuned via a dedicated test campaign.

4. MODEL-BASED VELOCITY ESTIMATION

Once the landing gear model is available, the model-based speed estimation is presented. Its structure, depicted in Fig. 6, consists of three interconnected blocks: the left and right wheel observers – devoted to the estimate of the left and right longitudinal forces – and a last block which finalizes the computation of the estimated velocity.

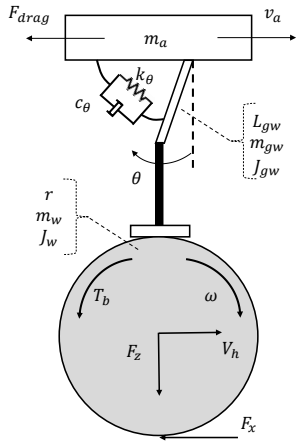

Fig. 5. Schematic representation of an aircraft landing gear.

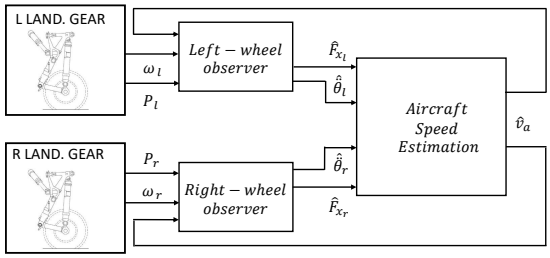

Fig. 6. Block-diagram of the model-based speed estimation algorithm.

The two wheel observers are structurally identical, featuring as measured inputs the applied pressure and the rotational speed of the corresponding wheel; moreover the estimated aircraft velocity enters the observers *via* a feedback loop from the speed estimation block. As detailed in Tanelli et al. (2012) they are SM observers based on the (non-true) assumption that the wheel speed cannot be measured and using the wheel speed estimation error as sliding variable:

$$s_{\omega_i} = \omega_i - \hat{\omega}_i,$$

where $\hat{\omega}_i$ represents the estimated rotational speed and $i = \{l, r\}$, stands for left and right. The control signal of the sliding mode observer is defined as

$$\Omega_i = K_i \text{sign}(s_{\omega_i}),$$

where K_i is the tunable observer gain. Within this setting, the estimated wheel speed dynamics take the form

$$\dot{\hat{\omega}}_i = \frac{1}{J_w}(\Omega_i - T_{b_i})$$

where the braking torque T_{b_i} is obtained from the measured pressure P_i through a static map that depends on the brake actuator characteristics. To ensure finite time reaching of the sliding manifold, that is

$$t_{reach_i} \leq \frac{|s_{\omega_i}|}{\epsilon},$$

it must hold that

$$s_{\omega_i} \dot{s}_{\omega_i} <= -\epsilon |s_{\omega_i}|, \quad (4)$$

where $\epsilon \in R^+$ and $\dot{s}_{\omega_i}$ can be expressed as

$$\dot{s}_{\omega_i} = \dot{\omega}_i - \dot{\hat{\omega}}_i = \frac{r F_{x_i} - K \text{sign}(s_{\omega_i})}{J_w}.$$

If K_i is chosen large enough to ensure that

$$K_i \geq r \max_{\lambda} F_{x_i} = r \max_{\lambda} F_{z_i} \mu(\lambda_i)$$

then condition (4) holds. Given the first-order SM nature of the observer, the control signal Ω_i is subject to chattering, and thus cannot be used in practice as is. The signal is thus low-pass filtered to yield the equivalent control signal Ω_{eq_i}. Note that the equivalent control signal Ω_{eq_i} is by construction capable of steering to zero the estimation error, *i.e.*,

$$\dot{s}_{\omega_i} = \frac{rF_{x_i} - \Omega_{eq_i}}{J_w}$$

and therefore it can be used to estimate the value of the $i-th$ tire-road contact force as

$$\hat{F}_{x_i} = \frac{\Omega_{eq_i}}{r}. \tag{5}$$

The estimated velocity $\hat{v}_a$ can then obtained from the expression of the longitudinal aircraft dynamic, which can be derived from from Equation (1), and has the form

$$\dot{\hat{v}}_a = \frac{1}{m_{tot}} \left(J_\theta \ddot{\hat{\theta}}_r + J_\theta \ddot{\hat{\theta}}_l - \hat{F}_{x_l} - \hat{F}_{x_r} - \alpha_d \hat{v}_a^2 \right). \tag{6}$$

In Equation (1) $\hat{F}_{x_l}, \hat{F}_{x_r}$ represent the estimated left and right longitudinal contact forces obtained by (5), respectively, while $\ddot{\theta}_l, \ddot{\theta}_r$ represent the gear walk angular acceleration and are computed from Equation (2) as

$$\ddot{\hat{\theta}}_i = \frac{1}{J_{\ddot{\theta}_i} - J_{\ddot{\theta}_i}^2 m_{tot}} \left[(L_{gw} - \frac{J_{\theta_i}}{m_{tot}}) \hat{F}_{x_i} - c_\theta \dot{\hat{\theta}}_i - k_\theta \hat{\theta}_i - \frac{J_{\theta_i}}{m_{tot}} \alpha_d \hat{v}_a^2 \right],$$

with $i = \{i, r\}$ indicate the left and right wheel, respectively.

As a matter of fact, the model-based approach requires reliable values of the aircraft physical parameters, and its performance also depends on the tuning of the observer gain. Recalling that, as shown in Table 1, the working conditions of the aircraft in the different braking maneuvers vary a lot – especially in terms of mass and vertical load variations – the observer (constant) parameter values are tuned with so to minimize the RMSE on the final estimated speed over all available maneuvers.

An example of the estimation performance in a landing case is shown in Fig. 7 where the real and the estimated velocity are compared; the speed and slip estimation errors are also detailed. The obtained performance are quite satisfactory, validating the idea of using of the estimated wheel slip in a closed-loop anti-skid controller.

A concluding remark is that the estimated vehicle speed is retrieved from (6) by integrating its right-hand side. Despite the native signals – wheel encoders and braking pressures – are not so prone to biases as accelerometer-based ones, yet the long duration of the braking maneuver in aircraft makes integration error accumulate, potentially degrading the overall estimation.

5. BLACK-BOX VELOCITY ESTIMATION

A different approach to the velocity estimation problem is the purely data-driven one. Such solution may help in compensating the variations of the unmeasurable parameters, which cannot be trivially extracted from the data, possibly yielding a more accurate estimate.

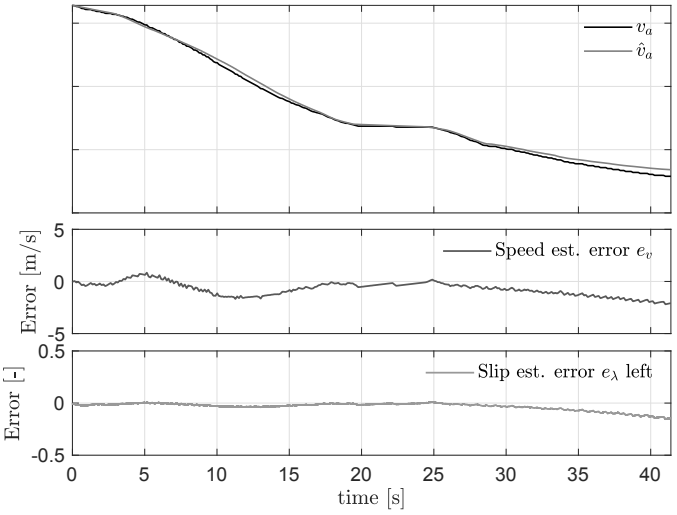

Fig. 7. Speed estimation performance of the model-based approach in landing maneuver.

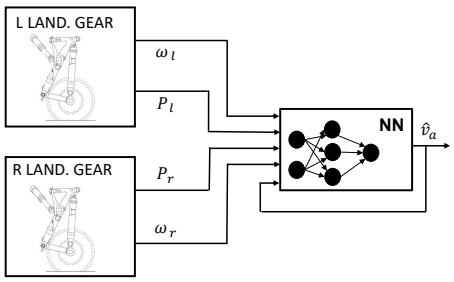

Fig. 8. Block-diagram of the black-box speed estimation algorithm.

Among the several possibilities, the artificial Neural Networks (NNs) were chosen. In the light of a fair comparison between the approaches, the same I/O configuration of model-based estimator has been used (see Fig. 8). Considering the dynamic nature of the problem at hand, we decided to use a nonlinear auto-regressive network with exogenous inputs (NARX) (Jain and Medsker, 1999). The defining equation of such model is

$$y(k) = f(y(k-1), .., y(k-n_y), u(k-1), .., u(k-n_u)),$$

where the value of the output signal at time $k \in \mathbb{N}$, *i.e.*, $y(k)$ is regressed on its past values along with present and past values of the exogenous input $u(k)$.

In the present case, the input signal $u(k)$ is defined as

$$u(k) = [\omega_l(k), \omega_r(k), P_l(k), P_r(k)]^T$$

with $\omega_l(k)$, $\omega_r(k)$, $P_l(k)$ and $P_r(k)$ being the left and right rotational speeds and the left and right pressures samples at time k, respectively.

The selected NARX structure features two layers. The hidden one has N neurons, each fed by the components of the input vector $u(k)$ and the estimated velocity $\hat{y}(k) = \hat{v}_a(k)$, delayed by d samples. All the resulting signals enter the $j-th$ neuron in a ridge construction mechanism:

$x_j(k) = w_{1,j} u_1(k) + \cdots + w_{d,j} u_1(k-d) + \cdots + w_d \hat{y}(k-d) + b_j$

where $w_{i,j}$, $i = 1, \ldots, d$ and b_j represent the weights and the bias of the $j-th$ neuron. The output layer shares the same construction mechanism applied to the output of the neurons of the hidden layer and, through the activation

function computes the velocity estimate $\hat{y}(k)$. The log-sigmoid activation function ($f(x) = \text{logsig}(x)$) has been used both for the hidden and the output layer.

The training phase was carried out using the series-parallel architecture, (Narendra and Parthasarathy, 1991), and the Bayesian regularization back-propagation method, see *e.g.* Rumelhart et al. (1988) and MacKay (1992).

The NN is completely defined once the amount of delay d and the number of neurons N in the hidden layer are fixed. To find the best NN structure, different delay/neurons combinations have been considered. In particular, given the limited number of experiments and after some preliminary testing, a $[3 \times 3]$ grid has been explored with $d \in [2, 3, 4]$ and $N \in [4, 5, 6]$, for a total of 9 possible NN structures. To find the best one, a leave-one-out cross-validation on the available maneuvers has been performed: the overall MSE is depicted in Fig. 9, leading to the selection of the $3D - 5D$ configuration as the optimal one.

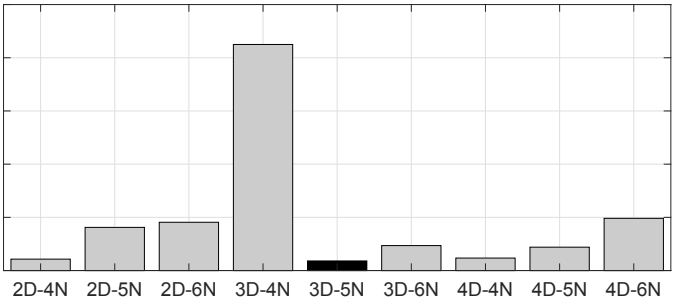

Fig. 9. Mean Square Error for the tested NN configurations.

Once defined the NN structure, among the 9 trained NNs the one providing the smallest validation error has been selected: the time domain results of the selected NN on its validation maneuver (a landing one) is depicted in Fig. 10. Also in this case the obtained performance is quite satisfactory, and again we can state that it is such as to allow the use of the estimated wheel slip in a closed-loop anti-skid controller.

6. COMPARED PERFORMANCE ANALYSIS

The performance comparison between the model-based and the black-box approach is here addressed. To do this the SM observer configuration which provides the best average performance on the whole data set is tested against the best NN model previously discussed. Fig 11 shows the estimated velocities obtained with the two approaches, along with the speed estimation errors. As can be seen, both methods result in a similar velocity profile, even though the black-box one shows more accurate estimation results especially in the last part of the maneuver (it's worth recalling how the SM approach suffers from the accumulation of integration errors).

Fig. 12 shows a quantitative comparison of the RMSE obtained by both methods on the entire data set. It clearly shows that the performance of the black-box algorithm does not significantly vary with the considered maneuver, and the RMSE is within $[0.9, 2.1] m/s$ in the whole set. As

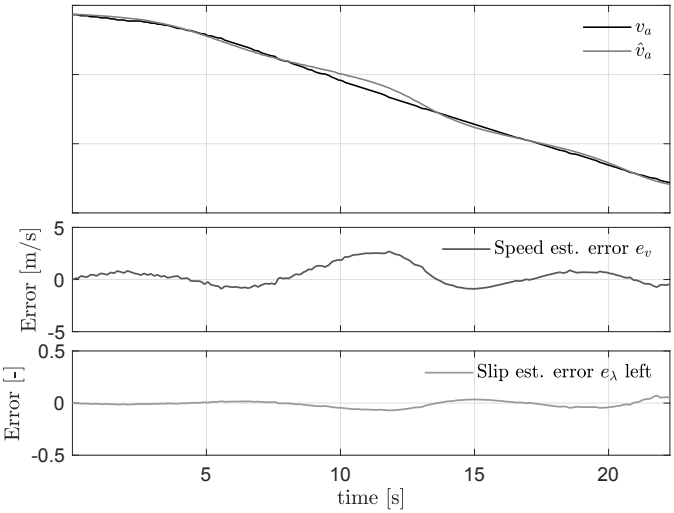

Fig. 10. Speed estimation performance of the black-box approach in landing maneuver.

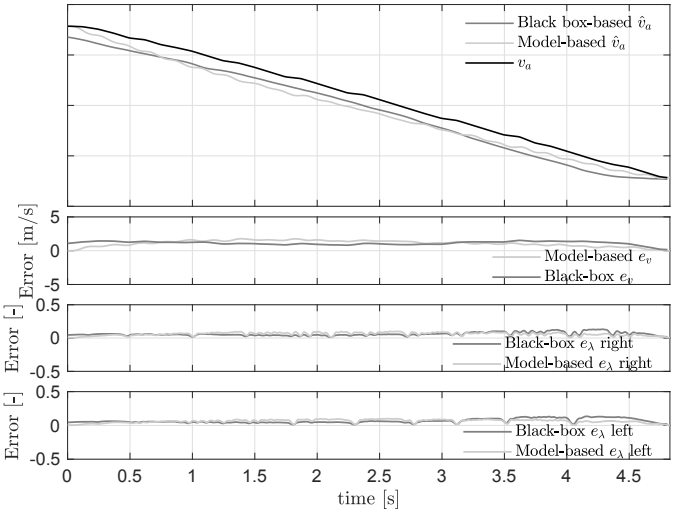

Fig. 11. Comparison of the speed estimation performance of the two estimation approaches in landing maneuver.

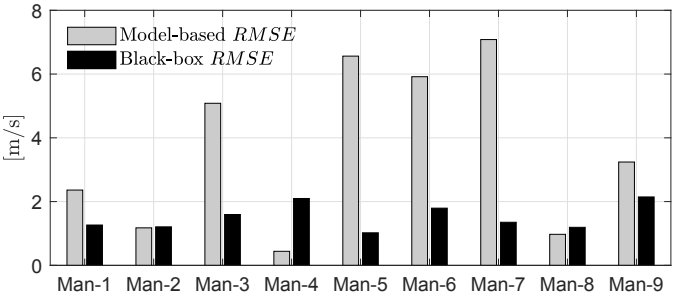

Fig. 12. RMSE of the two approaches computed over the whole data-set.

a matter of fact, the model-based solution suffers from the very high variability in the working conditions. In particular, maneuvers $3, 5, 6, 7$ result to be critical for the SM observer: these are the cases where the real mass of the aircraft is considerably different from that used for the estimation. Mass, in fact, resulted to be the most critical parameter as far as the model-based performance

is concerned. This being said, when the mass parameter used in the SM observer is close to the real one, the estimation error of the model-based approach results to be comparable or even lower than the one obtained with the black-box approach.

To further appreciate such fact, Fig 13 shows the speed estimates obtained on landing maneuvers with different mass values. The results confirm that when the mass value used in the observer is plausible the velocity estimation is very precise, while performance gradually degrades as the knowledge of the mass parameter worsens. On the one hand this encourages us to work on mass-estimation algorithms to improve the SM observer performance, but also witnesses an intrinsic larger robustness yielded by the black-box methods, which of course needs to be investigated over a larger experimental data set.

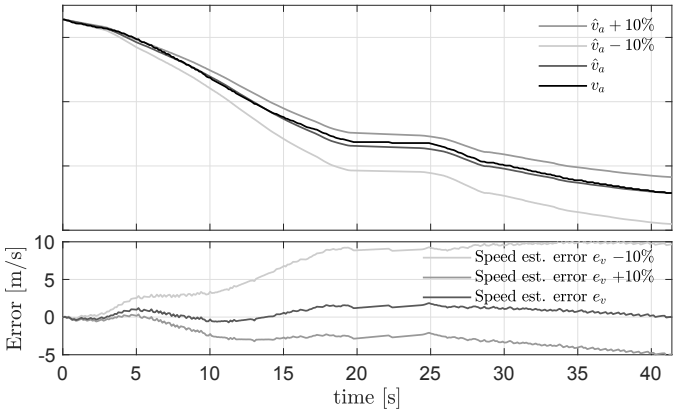

Fig. 13. Mass sensitivity of the model-based approach on a landing maneuvre.

7. CONCLUDING REMARKS

In this work the aircraft speed estimation is tackled, using the wheel speeds and the braking pressures, which are the sole signals available on the landing gear where the braking control unit is located. A comparison between model-based and black-box approaches for the estimation of aircraft speed is presented. Specifically, the model-based approach relies on a sliding-mode observer and the black-box approach, instead, on recurrent NNs. The analysis – performed on real aircraft data measured in landings and rejected take-off maneuvers – show that the model-based approach, while being preferable due to the possible formal analysis of the estimation properties, suffers from a very large set of operating conditions which cause significant parameters variations. Opposite, the black-box one seems inherently more robust in coping with the uncertainties, but requires to be paired with additional methods to test its integrity over the life cycle of the aircraft. Ongoing work is being devoted to evaluate the estimate for use in a slip-based anti-skid controller.

REFERENCES

Luis Alvarez, Jingang Yi, Roberto Horowitz, and Luis Olmos. Adaptive emergency braking control with observer-based dynamic tire/road friction model and underestimation of friction coefficient. *IFAC Proceedings Volumes*, 35(1):211–216, 2002.

Luca D'Avico, Mara Tanelli, Sergio Matteo Savaresi, M Airoldi, and G Rapicano. An anti-skid braking system for aircraft via mixed-slip-deceleration control and sliding mode observer. In *2017 IEEE 56th Annual Conference on Decision and Control (CDC)*, pages 4503–4508. IEEE, 2017.

Lakhmi C Jain and Larry R Medsker. *Recurrent neural networks: design and applications*. CRC Press, Inc., 1999.

Kazuyuki Kobayashi, Ka C Cheok, and Kajiro Watanabe. Estimation of absolute vehicle speed using fuzzy logic rule-based kalman filter. In *American Control Conference, Proceedings of the 1995*, volume 5, pages 3086–3090. IEEE, 1995.

Wolf R Krüger and Marco Morandini. Numerical simulation of landing gear dynamics: state-of-the-art and recent developments. *Proceedings of Limit Cycle Oscillation and Other Amplitude-Limited Self Excited Vibrations, RTO-MP-AVT-152, Loen, Norway*, 2008.

Reinhard Lernbeiss and Manfred Plöchl. Simulation model of an aircraft landing gear considering elastic properties of the shock absorber. *Proceedings of the Institution of Mechanical Engineers, Part K: Journal of Multi-body Dynamics*, 221(1):77–86, 2007.

David JC MacKay. Bayesian interpolation. *Neural computation*, 4(3):415–447, 1992.

Kumpati S Narendra and Kannan Parthasarathy. Learning automata approach to hierarchical multiobjective analysis. *IEEE Transactions on systems, man, and cybernetics*, 21(1):263–272, 1991.

Giulio Panzani, Matteo Corno, and SM Savaresi. Longitudinal velocity estimation in single-track vehicles. *IFAC Proceedings Volumes*, 45(16):1701–1706, 2012.

Laura R Ray. Nonlinear tire force estimation and road friction identification: Simulation and experiments. *Automatica*, 33(10):1819–1833, 1997.

David E Rumelhart, Geoffrey E Hinton, Ronald J Williams, et al. Learning representations by back-propagating errors. *Cognitive modeling*, 5(3):1, 1988.

Sergio M. Savaresi and M. Tanelli. *Active Braking Control Systems Design for Vehicles*. Springer-Verlag, London, UK, 2010.

Sergio M. Savaresi, M. Tanelli, and C. Cantoni. Mixed slip-deceleration control in automotive braking systems. *ASME Journal of Dynamic Systems, Measurement and Control*, 129(1):20–31, 2006.

S Semmler, D Fischer, R Isermann, R Schwarz, and P Rieth. Estimation of vehicle velocity using brake-by-wire actuators. *IFAC Proceedings Volumes*, 35(1): 169–174, 2002.

M. Tanelli, L. Piroddi, and Sergio M. Savaresi. Real-time identification of tire-road friction conditions. *IET Control Theory & Applications*, 3:891–906, 2009.

Mara Tanelli, Antonella Ferrara, and Paolo Giani. Combined vehicle velocity and tire-road friction estimation via sliding mode observers. In *Control Applications (CCA), 2012 IEEE International Conference on*, pages 130–135. IEEE, 2012.

Jingang Yi, Luis Alvarez, Xavier Claeys, and Roberto Horowitz. Emergency braking control with an observer-based dynamic tire/road friction model and wheel angular velocity measurement. *Vehicle system dynamics*, 39(2):81–97, 2003.